

Dipole emission and coherent transport in random media III. Emission from a real cavity in a continuous medium

M. Donaire^{1,*}

¹*Departamento de Física de la Materia Condensada,
Universidad Autónoma de Madrid, E-28049 Madrid, Spain.*

This is the third of a series of papers devoted to develop a microscopical approach to the dipole emission process and its relation to coherent transport in random media. In this paper, we compute the power emitted by an induced dipole and the spontaneous decay rate of a Lorentzian-type dipole. In both cases, the emitter is placed at the center of a real cavity drilled in a continuous medium.

PACS numbers: 42.25.Dd,05.60.Cd,42.25.Bs,42.25.Hz,03.75.Nt

It is known that the spontaneous emission rate, Γ , in a dielectric medium depends on the interaction of the emitter with the environment [1]. This is so because the surrounding medium determines the number of channels through which the excited particle can emit. That is, the local density of states (LDOS). For practical purposes the understanding of the spontaneous emission rate of a fluorescence particle is of great interest in biological imaging [2]. Closely related is the process of emission/reception by nano-antennas [3]. Also, inhibition of spontaneous emission is expected to occur in photonic band gap materials [4] as a signature of localization.

In a previous paper [5], general analytical formulae

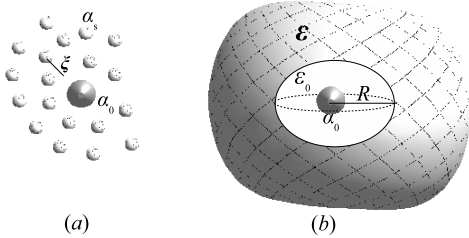


FIG. 1: (a) Cermet topology scenario. The emitter with polarizability α_0 is surrounded by a disconnected net of scatterers of polarizability α_s and correlation length ξ . (b) Simply-connected-non-contractible topology in which the emitter is placed at the center of a cavity of radius R surrounded by a continuous medium of dielectric contrast ϵ .

were derived for LDOS and Γ as functions of both the electrical susceptibility of the medium and the geometry of the embedding of the emitter in it. There, three different cases are addressed attending to the nature of the emitter. In the first case, the emitter is a polarizable dipole of transition amplitude μ at resonance. In the second case, the emitter is a non-resonant dipole of polarizability α with induced dipole moment $\epsilon_0 \alpha \vec{E}_0$, where \vec{E}_0 is a fixed exciting field. In the third case, the emitter is a fluorescent particle seated on top of a polarizable host particle. Attending to the embedding of the emitter and the topology of the system emitter-host-medium, we differentiated two cases [5]. In the first one, the emit-

ter is equivalent, replaces or is placed on top of a host scatterer. In such a case, by consistency, the topology of the medium is that of a disconnected manifold –known also as *cermet topology*– in the sense that the medium is made of spherical inclusions and the emitter takes the place of one of those inclusions. Attending to the embedding, the emitter is placed within a virtual cavity but for the case it replaces a host scatterer. The spatial correlation of the emitter with the surrounding medium is given by the same correlation function which enters the electrical susceptibility tensor, $\bar{\chi}$. Spatial dispersion in $\bar{\chi}$ is inherent to that topology. This scenario was studied in [6] with an emitter seated on top of a host scatterer. A relation between the complex refraction index of the host medium and the spontaneous decay rate was found.

In this paper we will focus on the remaining topological case. The emitter is seated at the center of a spherical cavity drilled in a homogeneous medium. This medium is continuous as seen by the emitter provided that the cavity radius, R , is much larger than any correlation length between the constituents of the host medium, ξ . Thus, the cavity is real. On the other hand, if the wavelength of the emitted field, λ , is that long that it cannot resolve neither the microscopical structure of the medium nor the cavity, the medium is also continuous as seen by the propagating field. Consequently, the host medium is characterized by a scalar susceptibility χ which does not present spatial dispersion. Topologically, this setup corresponds to that of a simply-connected-non-contractible manifold with a unique hollow sphere –see Fig.1. Regarding the emitter nature, two scenarios will be addressed for their potential interest in biological imaging and signal processing. In the first one, the emitter will be a polarizable particle excited by an external fixed field of frequency much lower than any of the resonance frequencies of the emitter. The physical quantity to compute in this case will be the power emission, W^α . In the second case, the emitter will be a polarizable particle which decays at some resonance frequency. Dipole induction will be encoded in the emitter itself as it will be assumed to be of Lorentz-type. Thus, the net effect of the host medium will reflect on a variation in the spontaneous decay rate,

Γ^α , together with a shift in the resonance frequency with respect to those values in free space.

In the first scenario, the formula for the power emitted by an induced dipole reads

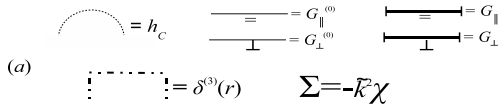
$$\begin{aligned} W^\alpha &= \frac{\omega_0 \epsilon_0^2}{2} \Im \left\{ \frac{\alpha_0}{1 + \frac{1}{3} k_0^2 \alpha_0 [2\gamma_\perp + \gamma_\parallel]} \right\} |E_0^\omega|^2 \quad (1) \\ &= \frac{-\omega_0^3 \epsilon_0^2}{6c^2} \left[\frac{|\alpha_0|^2}{|1 + \frac{1}{3} k_0^2 \alpha_0 [2\gamma_\perp + \gamma_\parallel]|^2} \Im \{ 2\gamma_\perp + \gamma_\parallel \} \right. \\ &\quad \left. - \frac{\Im \{ \alpha_0 \}}{|1 + \frac{1}{3} k_0^2 \alpha_0 [2\gamma_\perp + \gamma_\parallel]|^2} \right] |E_0^\omega|^2, \quad (3) \end{aligned}$$

where ω_0 is the frequency of the exciting field \vec{E}_0^ω , with $k_0 = \omega_0/c$ much lower than any internal resonance frequency and $\alpha_0 \equiv 4\pi a^3 \frac{\epsilon_e - 1}{\epsilon_e + 2}$ is the electrostatic polarizability of the emitter in vacuum, being $\epsilon_e(\omega_0)$ its dielectric contrast and a its radius. For our topological setup, the γ -factors $\gamma_{\perp, \parallel}$ are given by [5]

$$\begin{aligned} 2\gamma_\perp(\tilde{k}) &= -i \frac{\tilde{k}}{2\pi} - 2\tilde{k}^2 \int \frac{d^3 k}{(2\pi)^3} [C_\perp + G_\perp^{(0)}] \chi_\perp G_\perp^{(0)}(k) \\ &\quad + 2\tilde{k}^4 \int \frac{d^3 k}{(2\pi)^3} [C_\perp + G_\perp^{(0)}]^2 G_\perp \chi_\perp^2(k), \quad (4) \end{aligned}$$

$$\begin{aligned} \gamma_\parallel(\tilde{k}) &= -\tilde{k}^2 \int \frac{d^3 k}{(2\pi)^3} [C_\parallel + G_\parallel^{(0)}] \chi_\parallel G_\parallel^{(0)}(k) \\ &\quad + \tilde{k}^4 \int \frac{d^3 k}{(2\pi)^3} [C_\parallel + G_\parallel^{(0)}]^2 G_\parallel \chi_\parallel^2(k), \quad (5) \end{aligned}$$

with \tilde{k} evaluated at k_0 and where the cavity factors $C_{\perp, \parallel}$ are

(a) 

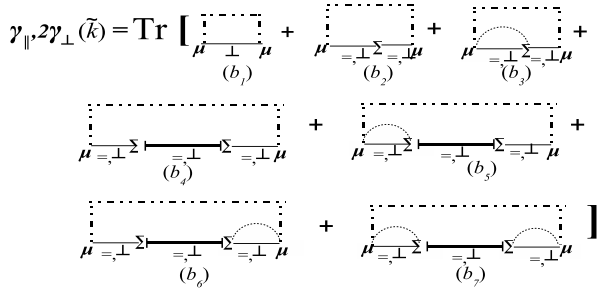
(b) 

FIG. 2: (a) Feynman's rules. (b) Diagrammatic representation of the transverse and longitudinal polarization factors, $2\gamma_\perp$ and γ_\parallel , as given by Eqs.(4,5).

$$\begin{aligned} C_\perp(k) &= \frac{1}{2} \int d^3 r e^{i\vec{k}\cdot\vec{r}} h_C(r) \text{Tr} \{ \bar{G}^{(0)}(r) [\bar{I} - \hat{k} \otimes \hat{k}] \} \\ &= \frac{1}{2} \int \frac{d^3 k'}{(2\pi)^3} h_C(|\vec{k}' - \vec{k}|) \left[G_\perp^{(0)}(k') \right. \\ &\quad \left. + G_\perp^{(0)}(k') \cos^2 \theta + G_\parallel^{(0)}(k') \sin^2 \theta \right], \quad (6) \end{aligned}$$

$$\begin{aligned} C_\parallel(k) &= \int d^3 r e^{i\vec{k}\cdot\vec{r}} h_C(r) \text{Tr} \{ \bar{G}^{(0)}(r) [\hat{k} \otimes \hat{k}] \} \\ &= \int \frac{d^3 k'}{(2\pi)^3} h_C(|\vec{k}' - \vec{k}|) \\ &\quad \times \left[G_\parallel^{(0)}(k') \cos^2 \theta + G_\perp^{(0)}(k') \sin^2 \theta \right], \quad (7) \end{aligned}$$

with $\cos \theta \equiv \hat{k} \cdot \hat{k}'$. In these equations, $h_C(k)$ is the Fourier transform of the correlation function which describes the isolation of the emitter within a real cavity. For a spherical cavity of radius R , $h_C(r) = -\Theta(r - R)$. In the above equations G_\perp and G_\parallel are respectively the transverse and longitudinal components of the renormalized propagator of the coherent –macroscopic– electric field in the host medium. They read, $\bar{G}_\perp(k) = \frac{\Delta(\hat{k})}{\tilde{k}^2 \epsilon_\perp(k) - k^2}$, $\bar{G}_\parallel(k) = \frac{\hat{k} \otimes \hat{k}}{k^2 \epsilon_\parallel(k)}$, \hat{k} being a unitary vector along the propagation direction and $\Delta(\hat{k}) \equiv I - \hat{k} \otimes \hat{k}$ being the projective tensor orthogonal to the propagation direction. In these expressions, $\epsilon_{\perp, \parallel}(k) = 1 + \chi_{\perp, \parallel}(k)$. Because no spatial dispersion is assumed in the continuous medium, $\epsilon_\perp = \epsilon_\parallel \equiv \epsilon$ are functions of \tilde{k} only. $\bar{G}_{\perp, \parallel}^{(0)}$ are the components of the propagator of the electric field in free space with bare wave number \tilde{k} . They are given by the above formulae, $\bar{G}_\perp, \bar{G}_\parallel$, with $\epsilon_\perp = \epsilon_\parallel = 1$.

In the second scenario, the emitter nature differs from that in [6]. In the present case, the dipole moment of the emitter is not a linear combination of a fixed and an induced dipole. Rather than that, the emitter is polarizable in its own and its polarizability function $\alpha(\tilde{k})$ gets renormalized as a result of iterative self-polarization processes,

$$\alpha(\tilde{k}) = \alpha_0 \left[1 + \frac{1}{3} \alpha_0 \tilde{k}^2 \Re \{ 2\gamma_\perp^{(0)} \} + \frac{1}{3} \alpha_0 \tilde{k}^2 (2\gamma_\perp + \gamma_\parallel) \right]^{-1}. \quad (8)$$

In the above equation, the γ -factors are those in Eqs.(4,5). In addition, the term $\frac{1}{3} \alpha_0 \tilde{k}^2 \Re \{ 2\gamma_\perp^{(0)} \}$ has been introduced to account for the internal resonance of the emitter in vacuum. As shown in [7], it plays the role of a regulator of the intrinsic ultraviolet divergence in $G_\perp^{(0)}$. That is, $\Re \{ 2\gamma_\perp^{(0)} \} = \frac{-3}{k_0^2 \alpha_0}$, where α_0 is the corresponding real electrostatic polarizability and k_0 is the resonance wave number in vacuum. Following [8], by parametrizing Eq.(8) in a Lorentzian (L) form, $\alpha_L(\tilde{k}) = \alpha'_0 k_{res}^2 [k_{res}^2 - \tilde{k}^2 - i\Gamma^\alpha \tilde{k}^3 / (ck_{res}^2)]^{-1}$, we can iden-

tify the decay rate of the emitter in the host medium as

$$\begin{aligned}\Gamma^\alpha &= -\frac{c}{3}\alpha'_0\tilde{k}^3\Im\{2\gamma_\perp + \gamma_\parallel\}|_{\tilde{k}=k_{res}} \\ &= -\Gamma_0\frac{2\pi}{k_0^2}\tilde{k}\Im\{2\gamma_\perp + \gamma_\parallel\}|_{\tilde{k}=k_{res}},\end{aligned}\quad (9)$$

where k_{res} is a real non-negative root of the equation

$$(\tilde{k}/k_0)^2 - 1 = \frac{1}{3}\alpha_0\tilde{k}^2\Re\{2\gamma_\perp + \gamma_\parallel\}|_{\tilde{k}=k_{res}},\quad (10)$$

$\alpha'_0 = \alpha_0(k_0/k_{res})^2$ is the renormalized electrostatic polarizability and $\Gamma_0 = c\alpha_0 k_0^4/6\pi$ is the in-vacuum emission rate. As argued in [8], consistency with Fermi's golden rule requires $\alpha_0 = \frac{2|\mu|^2}{\epsilon_0\hbar ck_0}$, μ being the transition amplitude between two atomic levels in vacuum.

In view of Eqs.(1,2,3,9), we can address in parallel the computation of W^α and Γ^α for each scenario described above. The computation reduces to the evaluation of $2\gamma_\perp(\tilde{k}) + \gamma_\parallel(\tilde{k})$ for $\tilde{k} = k_0$ and $\tilde{k} = k_{res}$ respectively.

Following [5, 6], we will decompose Γ^α and W^α in transverse and longitudinal components, $\Gamma^\alpha = 2\Gamma_\perp^\alpha + \Gamma_\parallel^\alpha$ and $W^\alpha = 2W_\perp^\alpha + W_\parallel^\alpha$ respectively. Neglecting longitudinal resonances as in [6], only the transverse components contain propagating modes, Γ_P^α and W_P^α respectively, which are proportional to the coherent intensity and so to $\Im\{2\gamma_\perp^P(\tilde{k})\}$. It is convenient to identify their specific contribution to Γ^α and W^α for observational purposes in imaging. Propagating modes are those associated to complex poles of the propagators in the integrands of eq.(4). We can read their contribution from the diagrams in Fig.2,

$$\begin{aligned}\Im\{2\gamma_\perp^P(\tilde{k})\} &= 2\int\Im\{G_\perp(k)\}\frac{d^3k}{(2\pi)^3} \\ &- 2\tilde{k}^2\Re\{\chi C_\perp(\tilde{k})\}\int\Im\{G_\perp^{(0)}(k)\}\frac{d^3k}{(2\pi)^3} \\ &+ 2\tilde{k}^4\Re\{[\chi C_\perp(\tilde{k})]^2\}\int\Im\{G_\perp(k)\}\frac{d^3k}{(2\pi)^3} \\ &+ 4\tilde{k}^4\Re\{\chi C_\perp(\tilde{k})\}\int\Im\{G_\perp^{(0)}(k)\chi G_\perp(k)\}\frac{d^3k}{(2\pi)^3},\end{aligned}\quad (11)$$

where the first term on the *right hand side* (*r.h.s*) of Eq.(11) contains the contribution of bulk propagation –transverse components of diagrams (b_1), (b_2), (b_4) in Fig.2.

All the above integrals in Eqs.(4-7,11) can be performed analytically at any order in $\tilde{k}R$. However, for the sake of consistency with the approximations considered so far, we take the limit $\tilde{k}R \ll 1$ and keep leading order terms,

$$\begin{aligned}2\gamma_\perp + \gamma_\parallel &\simeq -\frac{i}{2\pi}\tilde{k}\left[\left(\frac{\epsilon+2}{3}\right)^2\sqrt{\epsilon} - \frac{4(\epsilon-1)^2}{9\epsilon}\right] \\ &- \frac{\tilde{k}}{2\pi}\left[\left(\frac{1}{(\tilde{k}R)^3} + \frac{1}{\tilde{k}R}\right)\left[(\epsilon-1)\frac{\epsilon+2}{3\epsilon}\right]\right].\end{aligned}\quad (12)$$

It is our choice to normalize W^α to the propagating power in vacuum, $W_0 = \frac{\omega_0^4\epsilon_0^2}{12\pi c^3}\frac{|\alpha_0|^2}{|1-\frac{2}{6\pi}k_0^3\alpha_0|^2}|E_0^\omega|^2$. Thus, W^α reads

$$\begin{aligned}W^\alpha &= W_0\mathcal{R}_p(\alpha_0)\left[\Re\left\{\left(\frac{\epsilon+2}{3}\right)^2\sqrt{\epsilon}\right\} - \frac{4}{9}\Re\left\{\frac{(\epsilon-1)^2}{\epsilon}\right\}\right. \\ &- \left.\left(\frac{1}{(k_0R)^3} + \frac{1}{k_0R}\right)\Im\left\{\frac{2(\epsilon-1)^2}{3\epsilon} - (\epsilon-1)\right\}\right. \\ &\left.+ \Im\{\alpha_0\}\right],\end{aligned}\quad (13)$$

$$\begin{aligned}&- \left(\frac{1}{(k_0R)^3} + \frac{1}{k_0R}\right)\Im\left\{\frac{2(\epsilon-1)^2}{3\epsilon} - (\epsilon-1)\right\} \\ &+ \Im\{\alpha_0\}],\end{aligned}\quad (14)$$

$$\quad (15)$$

where $\mathcal{R}_p(\alpha_0) = |1 + \frac{1}{3}k_0^2\alpha_0[2\gamma_\perp(k_0) + \gamma_\parallel(k_0)]|^{-2}$ is the renormalization factor due to self-polarization cycles. Written this way, we recognize in the first term of the *r.h.s* of Eq.(13) the usual bulk term corrected by Lorentz-Lorenz (LL) local field factors [10], $\Gamma^{LL} = \Gamma_0\Re\left\{\left(\frac{\epsilon+2}{3}\right)^2\sqrt{\epsilon}\right\}$. The second term there includes corrections of order $\gtrsim \chi^2$. It is also remarkable that if the empty-cavity Onsager–Böttcher (OB) [14, 17] local field factors are used instead, $\Gamma^{OB} = \Gamma_0\Re\left\{\left(\frac{3\epsilon}{2\epsilon+1}\right)^2\sqrt{\epsilon}\right\}$ does agree with the two terms of Eq.(13) up to order χ^2 . The terms in Eq.(14) are associated to absorption in the host medium [6, 11] while that in Eq.(15) corresponds to absorption in the emitter. The propagating emission reads

$$\begin{aligned}W_P^\alpha &= W_0\mathcal{R}_p(\alpha_0)\Im\{2\gamma_\perp^P(k_0)\} \\ &= W_0\mathcal{R}_p(\alpha_0)\left[\Re\{\sqrt{\epsilon}\}\Re\left\{\left(\frac{\epsilon+2}{3}\right)^2\right\}\right. \\ &- \left.\frac{1}{3}\Re\{\epsilon-1\}\right].\end{aligned}\quad (16)$$

As shown in [6] at leading order, the second term in Eq.(16) subtracts from the total Γ^{LL} the non-propagating, non-absorptive longitudinal contribution.

It is worth comparing this result with that obtained in [6]. There, provided that ϵ follows Maxwell-Garnett (MG) formula [9] and neglecting absorption,

$$W_P^{MG} \simeq W_0\mathcal{R}_p^{MG}(\alpha_0)\left[\Re\{\sqrt{\epsilon}\}\Re\left\{\frac{\epsilon+2}{3}\right\}\right].\quad (17)$$

Eq.(16) and Eq.(17) agree at leading order in χ . However, in [6] the cermet topology was considered and the emitter was placed at the site of one of the host scatterers. The coincidence of both approaches at leading order bases on the fact that the limit $k_0\xi \ll 1$, with ξ being the radius of the exclusion volume between host scatterers, is implicit in Eq.(17). Therefore, no spatial dispersion enters χ – hence, MG holds – and the radius of the virtual cavity $R = \xi$ also satisfies $k_0R \ll 1$ as in the present case.

It is straightforward to write W_P^α in function of the effective refraction index \bar{n} and the extinction coefficient $\kappa \equiv (2k_0l_{ext})^{-1}$, with l_{ext} the extinction mean free path, using the identities $\Re\{\chi\} = \bar{n}^2 - 1 - \kappa^2$ and $\Im\{\chi\} = 2\bar{n}\kappa$,

$$\begin{aligned}W_P^\alpha &= W_0\mathcal{R}_p(\alpha_0)\left[\frac{\bar{n}}{9}(4 + \bar{n}^4 + \kappa^4 - 6\bar{n}^2\kappa^2 + 4\bar{n}^2 - 4\kappa^2)\right. \\ &- \left.\frac{1}{3}(\bar{n}^2 - 1 - \kappa^2)\right].\end{aligned}\quad (18)$$

For the sake of completeness, we give also the values of the non-propagating emission in terms of \bar{n} , κ and α_0 ,

$$W_{NP}^\alpha = W_0 \mathcal{R}_p(\alpha_0) \left\{ \Im\{\alpha_0\} \right. \quad (19)$$

$$+ \left[\frac{2\kappa^2 \bar{n}}{9} \left(1 - \frac{4}{(\kappa^2 + \bar{n})^2} \right) \right] \quad (20)$$

$$+ \frac{2\bar{n}\kappa}{3} \left(\frac{1}{(k_0\xi)^3} + \frac{1}{k_0\xi} \right) \left(1 + \frac{2}{(\bar{n}^2 + \kappa^2)^2} \right) \\ + \frac{5}{9} \left(1 + \frac{\kappa^6 - \bar{n}^6 + (\kappa^2 - \bar{n}^2)(4 - \kappa^2 \bar{n}^2)}{5(\kappa^2 + \bar{n}^2)^2} \right) \left. \right\} \quad (21)$$

where Eqs.(19,20,21) correspond to the power absorbed by the emitter, the transverse non-propagating power, W_{\perp}^{NP} , and the longitudinal emission, W_{\parallel}^α , respectively. Further on, by invoking causality, Kramers-Kronig sum rules relate \bar{n} and l_{ext} and variations of W^α can be obtained as a function of ω_0 [12].

Let us introduce next the self-polarization effect. This is done by multiplying all the expressions above for W^α by the renormalization factor $\mathcal{R}_p(\alpha_0)$. Neglecting absorption both in the emitter and in the host medium, we obtain at leading order in k_0R ,

$$\mathcal{R}_p(\alpha_0) \simeq \left(1 - \frac{2}{3} \frac{\alpha_0}{V_R} \frac{\epsilon - 1}{3\epsilon} \frac{\epsilon + 2}{3} \right)^{-2}, \quad (22)$$

where V_R is the volume of the emitter cavity. In contrast, the OB renormalization factor due to self-polarization reads [8, 13, 14],

$$\mathcal{R}_p^{OB}(\alpha_0) = \left(1 - \frac{2}{3} \frac{\alpha_0}{V_R} \frac{\epsilon - 1}{3\epsilon} \frac{3\epsilon}{2\epsilon + 1} \right)^{-2}. \quad (23)$$

Eq.(22) and Eq.(23) differ just in the local field factor which multiplies $-\frac{2}{3} \frac{\alpha_0}{V_R} \frac{\epsilon - 1}{3\epsilon}$ in each expression. With this result we finalize the computation of W^α in the first scenario.

In the following, we address the scenario where the emitter is of Lorentzian kind and compute Eqs.(8-10). We first solve for the renormalized resonance wave vector k_{res} ,

$$k_{res} \simeq k_0 \left[1 - \frac{\alpha_0}{9V_R} \Re\left\{ (\epsilon - 1) \frac{\epsilon + 2}{3\epsilon} \right\} \right. \quad (24)$$

$$\left. + \frac{\alpha_0 k_0^3}{6\pi} \Im\left\{ \left(\frac{\epsilon + 2}{3} \right)^2 \sqrt{\epsilon} - \frac{4}{9} \frac{(\epsilon - 1)^2}{\epsilon} \right\} \right]. \quad (25)$$

At leading order in k_0R , the first two terms in Eq.(24) equal the expression found in [8] for an interstitial emitter. The additional terms in Eq.(25) are relevant for strongly absorptive media. That may be for instance the case of nano-antennas in metallic media [3]. Additional solutions to the one above for k_{res} are only admissible beyond the small cavity limit and/or the continuous medium approximation. That is, for $\tilde{k}R \gtrsim 1$ and/or $\tilde{k}\xi \gtrsim 1$, Eq.(10) may contain several real solutions. That might give rise to a splitting of the in-vacuum resonant

peak provided such an splitting is broader than the line width. The origin of the resonance shifts of Eqs.(24,25) is in the virtual photons which dress up the polarizability α through Eq.(8). Those photons trace closed spatial loops as depicted by the diagrams in Fig.(2). They amount to a classical continuum of states not to be confused with real localized photons. The resultant frequency shift must be rather interpreted as the classical analog to the quantum Lamb shift [15, 16]. On the other hand, the possibility of a resonance splitting would be subjected to consistency with our perturbative renormalization scheme and linear-response approximation.

Finally, we give the full expression for Γ^α at lowest order in k_0R according to Eq.(9),

$$\Gamma^\alpha \simeq \Gamma_0 \left[1 - \frac{2\alpha_0}{9V_R} \Re\left\{ (\epsilon - 1) \frac{\epsilon + 2}{3\epsilon} \right\} \right. \\ + \frac{2\alpha_0 k_0^3}{6\pi} \Im\left\{ \left(\frac{\epsilon + 2}{3} \right)^2 \sqrt{\epsilon} - \frac{4}{9} \frac{(\epsilon - 1)^2}{\epsilon} \right\} \\ \times \left[\Re\left\{ \left(\frac{\epsilon + 2}{3} \right)^2 \sqrt{\epsilon} - \frac{4}{9} \frac{(\epsilon - 1)^2}{\epsilon} \right\} \right. \\ \left. \left. + \left(\frac{1}{(k_0R)^3} + \frac{1}{k_0R} \right) \Im\left\{ (\epsilon - 1) \frac{\epsilon + 2}{3\epsilon} \right\} \right] \right]. \quad (26)$$

Eqs.(24-26) can be compared with the results of [8, 18].

In summary, following [5], we have found analytical expressions for the power emitted by an induced dipole W^α –Eqs.(13,14,15,22)– and for the spontaneous emission rate Γ^α of a Lorentzian-type emitter –Eqs.(9,26)– from a real cavity in a continuous medium. In the former case we compute both the propagating and non-propagating power emission –Eq.(18) and Eqs.(19-20) respectively– in function of the complex index of refraction. In the latter case, we also compute the shift in the resonance frequency k_{res} –Eqs.(10,24,25). We found that, in the small cavity limit, $\tilde{k}R \ll 1$, the tuning of k_{res} may be sensitively affected by a strongly absorptive metallic environment –Eq.(25). Beyond that limit and/or the continuous medium approximation, we argue on the possibility of obtaining additional resonance frequencies.

This work has been supported by Microseres-CM and the EU Integrated Project "Molecular Imaging" (LSHG-CT-2003-503259).

* Electronic address: manuel.donaire@uam.es

- [1] E.M. Purcell, Phys. Rev. **69**, 681 (1946).
- [2] K. Suhling, P.M. W. French and D. Phillips, Photochem. Photobiol. Sci. **4**, 13 (2005).
- [3] V.V. Protasenko, A.C. Gallagher, Nano. Lett. **4**, 1329 (2004); J.N. Farahani, D.W. Pohl, H.J. Eisler and B. Hecht, Phys. Rev. Lett. **95**, 017402 (2005); R. Carminati, J.J. Greffet, C. Henkel and J.M. Vigoureux, Opt. Com. **261** (368).
- [4] E. Yablonovitch, Phys. Rev. Lett. **58**, 2059 (1987); S. John, Phys. Rev. Lett. **58**, 2486 (1987); S. John and T.

- Quang, Phys. Rev. A **50**, 1764 (1994).
- [5] M. Donaire and J.J. Saenz, e-print arXiv:0811.0323.
- [6] M. Donaire, e-print arXiv:0811.0373.
- [7] P. de Vries, D.V. van Coevorden and A. Lagendijk, Rev. Mod. Phys. **70**, 447 (1998).
- [8] P. de Vries and A. Lagendijk, Phys. Rev. Lett. **81**, 1381 (1998).
- [9] A. Lagendijk *et al.* Phys. Rev. Lett. **79**, 657 (1997).
- [10] H.A. Lorentz, Wiedem. Ann. **9**, 641 (1880); L. Lorenz, Wiedem. Ann. **11**, 70 (1881).
- [11] S.M. Barnett, B. Huttner and R. Loudon, Phys. Rev. Lett. **68**, 3698 (1992); S.M. Barnett, B. Huttner, R. Loudon and R. Matloob, J. Phys. B **29**, 3763 (1996); L.S. Froufe-Perez, R. Carminati and J.J. Saenz, Phys. Rev. A **76**, 013835 (2007).
- [12] S.M. Barnett and R. Loudon, Phys. Rev. Lett. **77**, 2444 (1996); R. Carminati and J.J. Saenz, to appear in Phys. Rev. Lett. (2009).
- [13] F. Hynne and R.K. Bullough J. Phys. A **5**, 1272 (1972); F. Hynne and R.K. Bullough, Phil. Trans. R. Soc. Lond. A **321**, 305 (1987).
- [14] L. Onsager, J. Am. Chem. Soc. **58**, 1486 (1936); C.J.F.Böttcher, *Theory of Electric Polarization* Elsevier, Amsterdam (1973)
- [15] J.M. Wylie and J.E. Sipe, Phys. Rev. A **30**, 1185 (1984).
- [16] J.J. Sakurai, *Advanced Quantum Mechanics* Addison-Wesley (1973).
- [17] R. Glauber and M. Lewenstein, Phys. Rev. A **43**, 467 (1991).
- [18] M.Fleischhauer, Phys. Rev. A **60**, 2534 (1999).